Journal of the Korean Nuclear Society
Volume 19, Number 1, March, 1987

Out-of-Pile Test for Yielding Behavior of PWR Fuel Cladding Material

Jae-Kyung Yi and Byong-Whi Lee
Korea Advanced Institute of Science and Technology
(Received February 16, 1987)

노외 실험을 통한 가압경수형 핵연료 피복재의 항복거동연구

이 재 경·이 병 휘
한국과학기술원
(1987. 2. 16 접수)

Abstract

The confirmed integrity of nuclear fuel cladding materials is an important object during steady state and transient operations at nuclear power plant. In this context, the clad material yielding behavior is especially important because of pellet-clad gap expansion.

During the steep power excursion, the in-pile irradiation behavior differences between uranium-dioxide fuel pellet and zircaloy clad induce the contact pressure between them. If this pressure reaches the zircaloy clad yield pressure, the zircaloy clad will be plastically deformed. After the reactor power resumed to normal state, this plastic permanent expansion of clad tube give rise to the pellet-clad gap expansion.

In this paper, the simple mandrel expansion test method which utilizes thermal expansion difference between copper mandrel and zircaloy tube was adopted to simulate this phenomenon. That is, copper mandrel which has approximately three times of thermal expansion coefficient of zircaloy-4(PWR fuel cladding material) were used in this experiment at the temperature range from 400C to 700C. The measured plastic expansion of zircaloy outer radius and derived mathematical relations give the yield pressure, yield stress of zircaloy-4 clad at the various clad wall temperatures, the activation energy of zircaloy tube yielding, and pellet-clad gap expansion.

The obtained results are in good agreement with previous experimental results. The mathematical analysis and simple test method prove to be a reliable and simple technique to assess the yielding behavior and gap expansion measurement between zircaloy-4 tube and uranium-dioxide fuel pellet under biaxial stress conditions.

요 약

원자력 발전소에 있어서 정상가동 상태나 이상동작시에 핵연료 피복관의 건전성 확보와 연관하여 피복재의 항복거동은 중요한 문제이다.

급격한 출력상승 상황에서 이산화 우라늄 소결체와 피복관 사이의 노내 조사거동의 차이는 소결체와 피복관 사이에 Contact Pressure를 야기 시킨다. 만일 이 Contact Pressure가 Zircaloy 피복관의 Yield Pressure에 도달하면 피복관에는 영구변형이 일어난다. 이 변형은 원자로의 출력이 정상

상태로 회복 되더라도 존재하므로 소결체와 피복관 사이의 Gap을 증대시킨다.

이러한 상황을 묘사하기 위해 본 논문에서는 구리 Mandrel과 Zircaloy 사이의 열팽창 차이를 이용하는 Mandrel 팽창 실험을 실행했다. 실험 결과 측정된 Zircaloy 피복관의 외경 팽창치와 본 논문에서 유도된 수학적 관계식들을 이용하여 온도에 따른 Zircaloy 피복관의 내부항복압력과 항복응력, 피복재의 항복에 따른 핵연료 소결체와 피복관 사이의 Gap 증대를 구하고, 항복 거동에 따른 온도의 영향을 보기 위해 항복과정의 활성화 에너지를 구했다.

본 실험과 분석에서 얻어진 이들 결과들은 다른 실험 결과들과 상당히 일치 하였으며, 이것으로 볼때 본 논문에서 유도된 관계식들과 Mandrel 팽창 실험이 Zircaloy 피복관의 항복거동과 Gap Expansion 측정에 신뢰성이 있음을 알 수 있었다.

Nomenclature

a : original mandrel radius at room temperature(mm)

b : original zircaloy inner radius at room temperature(mm)

c : original zircaloy outer radius at room temperature(mm)

a' : changed mandrel radius by thermal expansion at temperature T_0(mm)

b' : changed zircaloy inner radius by thermal expansion at temperature T_0(mm)

c' : changed zircaloy outer radius by thermal expansion at temperature T_0(mm)

b'' : changed zircaloy inner radius by elastic and plastic deformation at temperature T_0(mm)

c'' : changed zircaloy outer radius by elastic and plastic deformation at temperature T_0(mm)

δ_I : expansion difference between copper mandrel and zircaloy clad at temperature T_0(mm)

δ_{II} : shrinkage allowance by the compatibility between copper mandrel and zircaloy clad at temperature T_0(mm)

A : constant

d : initial clearance between mandrel outer radius and zircaloy inner radius at room temperature(mm)

d_1 : total mandrel contraction by contact pressure at temperature T_0(mm)

d_2 : total zircaloy tube expansion by contact pressure at temperature T_0(mm)

d_e : radial contraction of mandrel by elastic deformation at temperature T_0(mm)

d_p : radial contraction of mandrel by plastic deformation which is negligible at this experiment

d_e^i : the expansion or contraction of zircaloy inner radius by elastic deformation at temperature T_0(mm)

d_e^o : the expansion or contraction of zircaloy outer radius by elastic deformation at temperature T_0(mm)

d_p^i : the expansion of zircaloy inner radius by plastic deformation at temperature T_0(mm)

d_p^o : the expansion of zircaloy outer radius by plastic deformation at temperature T_0(mm)

$\bar{d}_p^i$: the plastic expansion of zircaloy inner radius after cooling to room temperature (mm)

$\bar{d}_p^o$: the plastic expansion of zircaloy outer radius after cooling to room temperature (mm)

α_1 : thermal expansion coefficient of copper mandrel at the reference temperature of 298K(mm/mmK)

α_2 : thermal expansion coefficient of zircaloy clad at the reference temperature of 308 K(mm/mmK)

t_0 : thickness of zircaloy clad at T_0(mm)

t : thickness of zircaloy clad under contact

pressure and temperature T_0(mm)

Δt : change of zircaloy clad thickness by contact pressure at temperature T_0(mm)

E_1 : Young's modulus of copper mandrel (MPa)

E_2 : Young's modulus of zircaloy clad(MPa)

ν_1 : Poisson's ratio of copper mandrel

ν_2 : Poisson's ratio of zircaloy clad

T : temperature(K)

T_0 : test temperature(K)

T_{room} : room temperature(K)

T_m : melting temperature of copper(1356K)

ΔT : $T_0 - T_{room}$(K)

P : contact pressure of zircaloy tube at yield point(MPa)

σ_θ : hoop stress(MPa)

σ_r : radial stress(MPa)

σ_y : uniaxial yield stress of zircaloy(MPa)

σ_{eff} : effective stress of zircaloy tube(MPa)

E_θ : hoop strain(m/m)

E_r : radial strain(m/m)

E_z : axial strain(m/m)

ΔG : gap expansion deformation(mm)

$\Delta G_{(\%)}$: the percentage of gap expansion(%)

r : radius(mm)

r_0 : original ralidus at room temperature(mm)

u : displacement(mm/mm)

I : legth(mm)

R : gas constant, 8.3144J/°C mole

Q : activation energy of yielding process of zircaloy tube(KJ/mole)

I. Introduction

The occurrence of thermal transients at the nuclear power plant may impose severe thermal and mechanical stresses on the reactor components. These transient conditions include both those occurring durring normal operation, such as start up, shut down and power level change (load following operation), and those occurring as the result of a plant malfunction. The intensity of these induced stresses depends on the magnitude and the rate of temperature change of the coolant and on the variation of the rate of radiation-induced internal heat generation in the structure which, in turn, is affected by changes in the reactor power level.

The transient mechanical response of nuclear reactor fuel cladding has recentely attracted much attention in conjunction with the integrity of fuel elements during anticipated reactor transients. The cladding response under the loss of coolant accident (LOCA) and the pellet-clad ding interaction (PCI) mechanism followed by power ramp are fairly studied by many investigators.

Chung et al.[1,2] have studied the mechanical response of zircaloy-4 cladding under the simulated condition of LOCA. They have indicated that the present criteria, namely, total oxidation limit of 17% of the wall thickness and maximum cladding temperature of 1477K, are conservative.

The material properity under power cycle have also been studied by the EPRI[3] and Puill et al.[4] The ramp-temperature tests using uniaxial data, with an internal pressurization of 6.2 MPa to 9.6 MPa failed at temperature near 1033K.[3]

Load following operations typically require power excurtion or cool down of 5% full power per minute under the unprogrammed load follow[4] or a change 10% of full power per minute under the programmed load follow.[5] Anticipated consequences for the fuel rods under the power ramp have been analyzed. Fuel rods are submitted to two types of thermal-mechanical transients, which can be possibly combined:

-Local power ramps, provoking PCI when the gap between pellets and cladding is sufficiently closed up.

-Cyclic low-level stress-strain variations which could damage the cladding by fatigue.

The failure mechanism of zircaloy-4 tube under steady and transient state have been

believed as stress corrosion cracking (SCC) mechanism[6] by many investigators. however, Chung et. al. have introduced the radiation-induced ZrO_2 precipitations which cause brittle fracture by dislocation blockage.[7,8]

The design and operating remedies have been introduced in an attempt to alleviate the impact of PCI on plant capacity.[9] Design remedis have addressed the mechanical-chemical nature of PCI, namely the reduction of clad stresses, fuel temperature, and/or fission release. Operation remedies have emphasized the reduced severity of the duty cycle through less uses of control rods for achieving power maneuvers and power shaping. This remedy is expensive in view of output loss during the slow increase to high power. Therefore, there is a clear economic incentive for understanding the basic mechanisms of these cladding failure, in order that effective operational, design or material remedies can be developed.

During the severe thermal excursion, the fuel pellet diameter may become larger than the zircaloy inner diameter because of temperature distribution difference and in-pile irradiation behavior difference. Thus, the elastic and plastic deformation of zircaloy tube has to accommodate the expansion of fuel pellet. After the reactor power resumed to normal operation state, the plastic expansion expansion difference between fuel and zircaloy clad may cause fuel-pellet gap expansion. Under these conditions, the heat conduction of the gap is reduced. Then, the temperature of fuel-pellet center line is increased. And the undesireable phenomena in the fuel rod occur. (e.g. such as fuel melting, fission gas release, plennum gas pressure build up, etc.)

In this paper, the zircaloy tube yield pressure and yield stress, the activation energy of yielding of zircaloy tube, and the pellet-clad gap expansion are obtained by the mathematical analysis of the experimental data of simple mandrel thermal expansion test to simulate power excursion conditions mechanically.

II. Theoretical Basis

During the steep power excursion, the different in-pile irradiation behavior between zircaloy clad and uranium-dioxide fuel pellet induces the contact pressure between them.

For this experimental simulation, the uranium-dioxide pellet is replaced with large thermal expansion copper rod to induce high thermal contact pressure between mandrel and clad. The copper mandrel has approximately three times of thermal expansion coefficient of zircaloy clad. To calculate the desired values, several mathematical equations are derived. The data for copper mandrel[10] and zircaloy-4 tube[11] used for calculations are tabulated in table I. The deriving procedures are as follows;

II. 1. Yielding Contact Pressure

II. 1. 1. The expansion difference between

Table I Copper and Zircaloy-4 Data.

Thermal Expansion Coefficient α (mm/mm°C)	Copper	$\alpha=\{0.3+2.167\times10^{-3}\times(T-500)\}/\{100\times(T-298)\}$
	Zircaloy-4	$\alpha=(6.72\times10^{-6}T-2.07\times10^{-3})/(T-308)$
Young's Modulus E (Pa)	Copper	$E=\{117.24-3\times7\times(T/T-0.22)\}\times10^3$ for $T/T_m\leq0.5$ $E=\{111.4-3\times7\times(T/T_m-0.5)\}\times10^3$ for $T/T_m>0.5$
	Zircaloy-4	$E=\{9.900\times10^5-566.9\times(T-273)\}\times9.81\times10^{-4}$
Poisson's Ratio ν	Copper	0.33
	Zircaloy-4	$\nu=0.3303+8.376\times10^{-5}(T-273.15)$

mandrel and zircaloy clad.

The changed radius of solid copper mandrel by thermal expansion at temperature T_0 is;

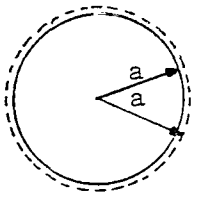

$$a'=a+\alpha_1 a\Delta T$$
$$=a(1+\alpha_1\Delta T) \quad (1)$$

Fig. 1. Changed Radius of Mandrel

The changed radius of zircaloy clad is also;

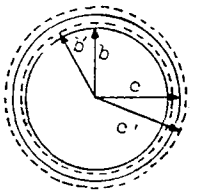

$$b'=b+\alpha_2 b\Delta T$$
$$=b(1+\alpha_2\Delta T) \quad (2)$$
$$c'=c+\alpha_2 c\Delta T$$
$$=c(1+\alpha_2\Delta T) \quad (3)$$

Fig. 2. Changed Radius of Zircaloy Tube

The initial clearance between copper mandrel and zircaloy tube is defined.

$$d=a-b \quad (4)$$

So the expansion difference between mandrel and clad at elevated furnace temperature T_0 is;

$$\delta_I=a'-b'$$
$$=(a-b)+(\alpha_1 a-\alpha_2 b)\Delta T$$
$$=d+(\alpha_1 a-\alpha_2 b)\Delta T \quad (5)$$

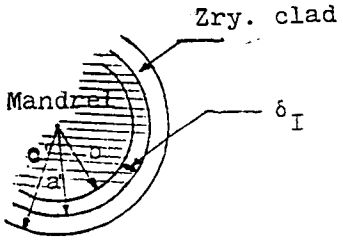

Fig. 3. Expansion Difference between Mandrel and Zircaloy Tube

II. 1. 2. Shrinkage allowance

The shrinkage allowance δ_{II} by the combination of mandrel and zircaloy tube at temperature T_0 is;

$$\delta_{II}=d_1+d_2$$
$$=d_e+d_e^i+d_p^i \quad (6)$$

where

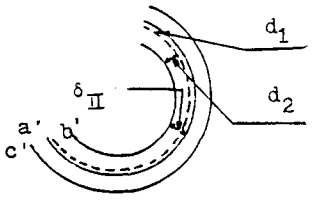

Fig. 4. Shrinkage Allowance

$$d_1=d_e+d_p$$
$$=d_e$$

and

$$d_2=d_e^i+d_p^i$$

Since copper mandrel was not deformed plastically during thermal expansion and contraction cycle throughout the experiment, therefore, $d_p=0$ in eq. (6).

To calculate d_p^i at eq. (6), the procedure using strain superposition is as follows;

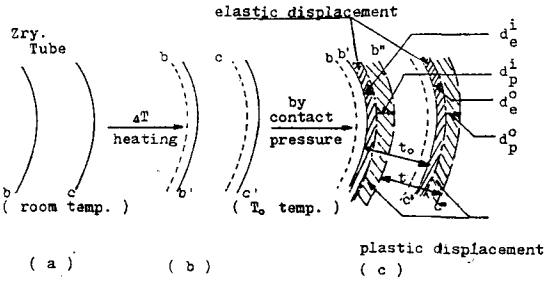

Fig. 5. Thickness Change Procedure

From Fig. 5, the thickness change of zircaloy clad by contact pressure at temperature T_0 is;

$$\Delta t=t-t_0$$
$$=(c''-b'')-(c'-b')$$
$$=(d_e^0+d_p^0)-(d_e^i+d_p^i) \quad (7)$$

So eq. (7) gives

$$d_p^i=d_e^0+d_p^0-d_e^i-\Delta t \quad (8)$$

Substituting eq. (8) into eq. (6);

$$\delta_{II}=d_e+d_e^0+d_p^0-\Delta t \quad (9)$$

This eq. (9) is composed of 4 terms. The first d_e and the second d_e^0 term depend on the contact pressure at the zircaloy tube yielding point. The third term d_p^0 is calculated from experimental

results $\bar{d}_p^0$ and the last term Δt is also calculated.

i) The relation between d_p^0 and $\bar{d}_p^0$ is

$$d_p^0=\frac{\bar{d}_p^0}{1-\alpha_2\Delta T} \tag{10}$$

ii) To calculate Δt, the followings are assumed; namely, the zircaloy tube is thin wall cylinder, the axial deformation is negligible, and the dilatation by elastic stress is negligible too.

Under the above assumptions, the strains are;

$$\epsilon_\theta=\ln\frac{r}{r_0}\simeq\ln\frac{c''}{c'} \tag{11}$$

$$\epsilon_r=\ln\frac{t}{t_0} \tag{12}$$

As the dilatation of plastic deformation is zero;

$$\epsilon_\theta+\epsilon_r+\epsilon_z=0 \tag{13}$$

From no axial deformation assumption, eq. (13) is

$$\epsilon_r=-\epsilon_\theta \tag{14}$$

Substituting eq. (11) and eq. (12) into eq. (14) gives

$$\ln\frac{t}{t_0}=\ln\frac{c'}{c''}$$

$$t=t_0\frac{c'}{c''}$$

$$=t_0\frac{c'}{c'+d_e^0+d_p^0}$$

$$=t_0\frac{1}{1+\frac{1}{c'}(d_e^0+d_p^0)}$$

$$=t_0\left\{1+\frac{1}{c'}(d_e^0+d_p^0)\right\}^{-1}$$

$$=t_0\left\{1-\frac{1}{c'}(d_e^0+d_p^0)\right\} \tag{15}$$

because of $(1+x)^{-1}\approx 1-x$ for $x\ll 1$

So the thickness change is;

$$\Delta t=t-t_0 \tag{16}$$

which is negative value.

Substituting eq. (15) into eq. (16);

$$\Delta t=-\frac{t_0}{c'}(d_e^0+d_p^0)$$

$$=-\frac{t_0}{c'}\left(d_e^0+\frac{\bar{d}_p^0}{1-\alpha_2\Delta T}\right) \tag{17}$$

Substituting eq. (10) and eq. (17) into eq. (9) gives;

$$\delta_{II}=d_e+d_e^0+d_p^0-\Delta t$$

$$=d_e+d_e^0+\frac{\bar{d}_p^0}{1-\alpha_2\Delta T}$$

$$+\frac{t_0}{c'}\left(d_e^0+\frac{\bar{d}_p^0}{1-\alpha_2\Delta T}\right)$$

$$=d_e+d_e^0\left(1+\frac{t_0}{c'}\right)$$

$$+\frac{\bar{d}_p^0}{1-\alpha_2\Delta T}\left(1+\frac{t_0}{c'}\right) \tag{18}$$

II. 1. 3. Yielding Pressure of Zircaloy Tube

The expanded radius of copper mandrel must be accommodated in the inner radius of zircaloy tube because of compatibility requirement between mandrel and zircaloy tube. This is shown in Fig. 3. and Fig. 4. So δ_I must be equal to δ_{II}, that is,

$$\delta_I=\delta_{II} \tag{19}$$

Substituting δ_I and δ_{II} into eq. (19);

$$d+(\alpha_1 a-\alpha_2 b)\Delta T$$

$$=d_e+d_e^0\left(1+\frac{t_0}{c'}\right)+\frac{\bar{d}_p^0}{1-\alpha_2\Delta T}\left(1+\frac{t_0}{c'}\right)$$

and rearrangement gives;

$$d_e+d_e^0\left(1+\frac{t_0}{c'}\right)$$

$$=d+(\alpha_1 a-\alpha_2 b)\Delta T-\frac{\bar{d}_p^0}{1-\alpha_2\Delta T}\left(1+\frac{t_0}{c'}\right) \tag{20}$$

To solve d_e and d_e^0 in eq. (20), the procedures using displacement equations[12] are as follows;

From $u=\frac{b^2\cdot p\cdot r}{E(b^2-a^2)}\left\{(1-\nu)+(1+\nu)\frac{a^2}{r^2}\right\}$

and for solid cylinder; $a=0$, $r=b=a'$,

$$d_e=\frac{p\cdot a'}{E_1}(1-\nu_1)$$

From $u=\frac{a^2\cdot p\cdot r}{E(b^2-a^2)}\left\{(1-\nu)+(1+\nu)\frac{b^2}{r^2}\right\}$

and for the present case, $a=b'$, $b=c'$, $r=c'$

$$d_e^0=\frac{1}{E_2}\cdot\frac{2b'^2c'p}{c'^2-b'^2}$$

$$d_e^j=\frac{b'^3\cdot p}{E_2(c'^2-b'^2)}\left\{(1-\nu_2)+(1+\nu_2)\frac{c'^2}{b'^2}\right\}$$

Substituting the above two eqs. into eq. (20);

$$P\left\{\frac{a'}{E_1}(1-\nu_1)+\frac{2}{E_2}\cdot\frac{b'^2c'}{c'^2-b'^2}\left(1+\frac{t_0}{c'}\right)\right.$$

$$=d+(\alpha_1 a-\alpha_2 b)\Delta T - \frac{\bar{d}_p^0}{1-\alpha_2\Delta T}\left(1+\frac{t_0}{c'}\right)\Big\} \quad (21)$$

Therefore eq. (21) gives the yield pressure of zircaloy tube;

$$P=\frac{d+(\alpha_1 a-\alpha_2 b)\Delta T-\frac{\bar{d}_p^0}{1-\alpha_2\Delta T}\left(1+\frac{t_0}{c'}\right)}{\frac{a'}{E_1}(1-\nu_1)+\frac{2}{E_2}\cdot\frac{b'^2c'}{c'^2-b'^2}\left(1+\frac{t_0}{c'}\right)} \quad (22)$$

II. 2. Stresses of Zircaloy tube

The hoop stress σ_θ of zircaloy tube is;

$$\sigma_\theta=\frac{p\cdot(b'+d_p^i)}{t_0+\Delta t} \quad (23)$$

The radial stress σ_r of zircaloy tube is;

$$\sigma_r=-\frac{p}{2} \quad (24)$$

The axial stress σ_z of zircaloy tube is;

$$\sigma_z=0 \quad (25)$$

because there is negligible friction between mandrel and zircaloy tube interphase in axial direction, therefore, no axial stress. From the effective stress definition;

$$\sigma_{\text{eff}}=\frac{1}{\sqrt{2}}\{(\sigma_\theta-\sigma_r)^2+(\sigma_r-\sigma_z)^2+(\sigma_z-\sigma_\theta)^2\}^{1/2} \quad (26)$$

and the effective stress of zircaloy tube at yield contact pressure under this experimental conditions is

$$\sigma_{\text{eff}}=-\frac{1}{\sqrt{2}}\{\sigma_2{}^\theta+\sigma_2{}^r+(\sigma_\theta-\sigma_r)^2\}^{1/2} \quad (27)$$

this may be equal to uniaxial tensile yield stress under Von-Mises theorem.

II. 3. Gap Expansion

The gap expansion by plastic deformation of zircaloy tube is as follows from eq. (8) and appropriate substitutions;

$$\Delta G=d_p^i$$
$$=d_e^0+d_p^z-\Delta t-d_e^i$$
$$=\frac{1}{E_2}\cdot\frac{2b'^2c'\cdot p}{c'^2-b'^2}+\frac{\bar{d}_p^0}{1-\alpha_2\Delta T}+\frac{t_0}{c'}\left(d_e^0+\frac{\bar{d}_p^0}{1-\alpha_2\Delta T}\right)-\frac{1}{E_2}\cdot\frac{b'^3\cdot p}{c'^2-b'^2}\left\{(1-\nu_2)+(1+\nu_2)\frac{c'^2}{b'^2}\right\} \quad (28)$$

By assuming that the pellet-clad gap is 0.2mm at the pressurized water reactor(PWR), the gap expansion percent by plastic deformation of zircaloy tube under these experimental conditions is;

$$G(\%)=\frac{\Delta G}{0.2}\times 100 \quad (29)$$

III. Experimental Procedure

III. 1. Materials

The zircaloy specimen used in this experiment was the commercially produced, stress-relieved SANDVIK zircaloy-4 tube with 25mm length. Its measured dimension is 9.480mm of inner diameter, 10.702mm of outer diameter, and 0.611mm of thickness.

Copper rod is commercially produced 99% copper and it was machined to 40mm length and various diameter size to 0.005mm accuracy to give differential initial clearance, d, value.

III. 2. Test Apparatus

The specimen set is composed with copper mandrel, zircaloy-4 clad, and chromel-alumel medium size thermocouple. They are shown in fig. 6 and 7. To reduce the initial copper mandrel diameter, liquid nitrogen is used. Then, copper mandrel is easily inserted into zircaloy tube. The heating system is composed with furnace and temperature controller.

III. 3. Procedures

The experimental procedures are as follows;

i. Set furnace at T_0 : 400, 450, 500, 600, and 700C.

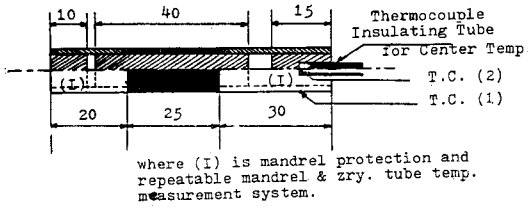

Fig. 6. Specimen Set Layout.

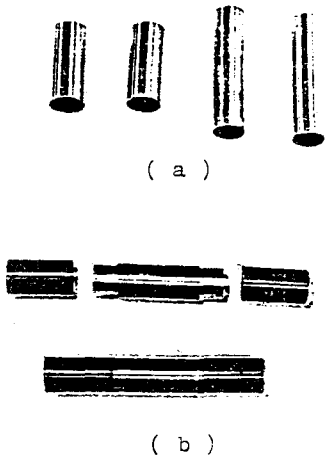

Fig. 7. Zircaloy-4 Cladding Tube Specimen and Copper Rod Mandrel (a) and Specimen Set without Thermocuple (b)

ii. Copper mandrel is inserted to zircaloy tube after mandrel diameter was reduced by liquid nitrogen.

iii. Mandrel, zircaloy tube, and mandrel protection and temperature measurement system are assembled.

iv. Assembled specimen set is put into the furnace and if T(1) and T(2) reach equal test temperature, it is air cooled to the room temperature.

v. Then, the outer diameter is measured by micrometer.

vi. The above process is repeated with different mandrel diameters and furnace temperatures.

As the result of these procedures, the plastic deformation of zircaloy tube was measured under variouss temperature and mandrel diameter combinations.

IV. Results and Discussion

The measured values of $\bar{d}_p^0$ are inserted into the derived equations. And the zircaloy tube yield pressure, yield stress, activation energy of yield process, and the percentage of the pellet-cladding gap expansion are calculated.

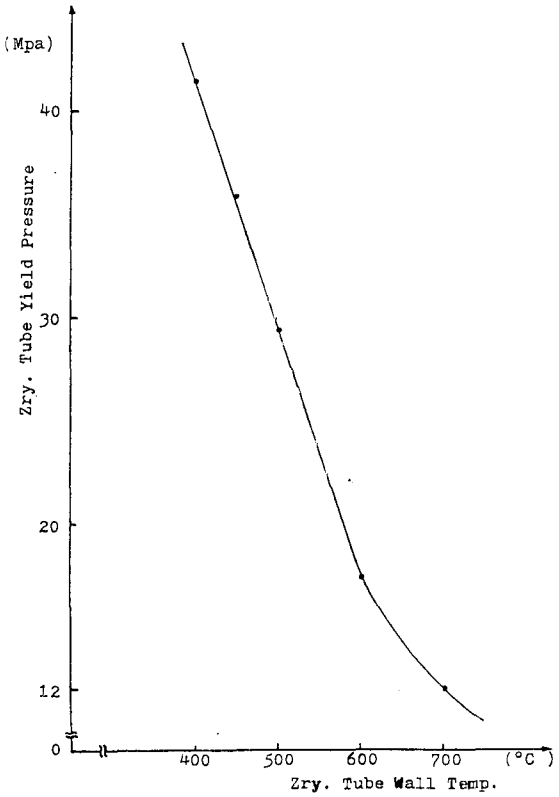

Fig. 8. Zircaloy Tube Yield Pressure vs. Tube Wall Temperature.

IV. 1. Zircaloy-4 Tube Yield Pressure versus Temperature.

By inserting the measured values of $\bar{d}_p^0$ into eq. (22), the zircaloy yield pressure is calculated. This yield pressure vs. zircaloy tube temperature is plotted in fig. 8. In this figure, the yield pressure of zircaloy tube decreases with temperature increase. The yield pressure decreases linearly at 400−600°C temperature range, whereas, above 600°C, the yield pressure decreases at lesser steep rate.

IV. 2. Effective Stress at yield pressure vs. Temperature.

As the yield pressure of zircaloy tube is calculated, the hoop stress, the radial stress, and the effective stress of the zircaloy tube are also calculated from eqs. in section II. 2. The effective stress in this case is equivalent with the uniaxial

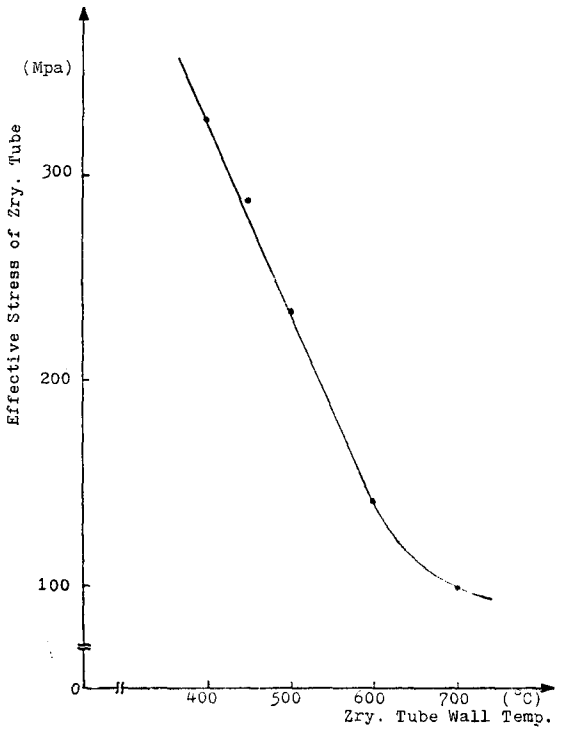

Fig. 9. Effective Stress of Zry. at Yield Pressure vs. Zry. Tube Wall Temperature.

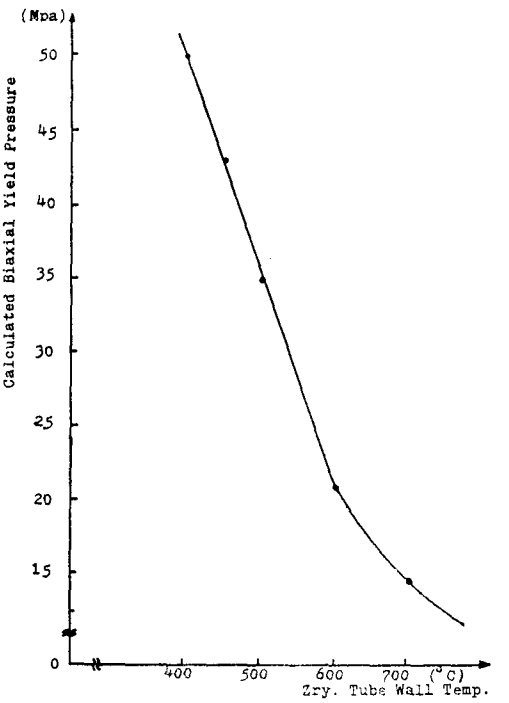

Fig. 10. Biaxial Yield Pressure by Internal Pressurization Method vs. Zry. Tube Wall Temperature

yield stress of zircaloy-4 tube at that temperature by Von-Mises yield theorem. So the uniaxial yield stress of zircaloy tube under this experimental conditions is plotted with zircaloy tube temperature in fig. 9. These yield stresses are well accorded with other experimental results or computer code results.[13] Therefore, the above all mathematical equations and experimental results are proven to be proper.

Using the above results of data, it is possible to guess the yielding pressure of zircaloy tube which is conducted internal gas pressurization test.[14]

Using eq. (26) and for the tube burst test, $\sigma_z=\sigma_\theta/2$ and $\sigma_r=0$ Substituting these stresses into the right hand side of eq. (26) gives

$$\sigma_{eff}=\frac{\sqrt{3}}{2}\sigma_\theta \tag{30}$$

To determine the internal gas pressure that should cause yielding of a closed tube, we set $\sigma_{eff}=\sigma_y$ and use the eq. (23) of hoop stress. Then eq. (30) gives;

$$P(\text{yielding})=\frac{2}{\sqrt{3}}\cdot\frac{t_0+\Delta t}{b'+d_p^i}\cdot\sigma y \tag{31}$$

The calculated yield pressure for tube burst test by eq. (31) is plotted in Fig. 10. These values fairly agree with other experimental results[15] for 400°C.

IV. 3. Activation Energy for Yield Process

The derived yield stress and pressure are strongly dependent upon the test temperatures. This phenomena is related with thermally activated deformation process at elevated temperature. The temperature dependence of flow stress is generally represented at constant strain and strain rate[16];

$$\sigma=A\exp(Q/RT)\,|\,\epsilon,\dot{\epsilon} \tag{32}$$

If this expression is obeyed, a plot of $\log\sigma$ versus $1/T$ will give a straight line with a slope $Q/2.303R$, that is,

$$\log\sigma=\log A+\frac{Q}{2.303R}\cdot\frac{1}{T} \tag{33}$$

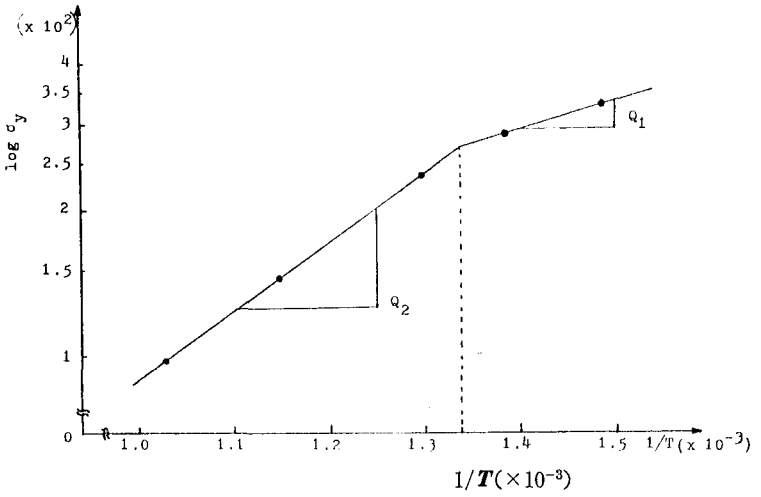

Fig. 11. Activation Energy of Zry-4 Tube Yielding along Tube Wall Temperature

For this experimental conditions, ϵ is the strain at the yielding point and $\dot{\epsilon}$ is given by

$$\dot{\epsilon}=\frac{\bar{d}_p^0/C}{\text{Specimen Heating Time}} \qquad (34)$$

where the calulated $\dot{\epsilon}$ by eq. (34) is nearly the order of 10^{-6}/sec for this experimental conditions.

Using these relations, the calculated log σ is poltted versus $1/T$ in fig. 11. The calculated Q values from the slope are

Q_1=10.75KJ/mole

for the temperature range of 400−474°C

Q_2=26.06KJ/mole

for the temperature range of 474−700°C

The activation energy of yielding process is changed near 474°C. Evidently, the mechanism of zircaloy tube yielding process is changed at that temperature.

IV. 4. The Expansion Percentage of Pellet-Cladding Gap versus the Percentage of Mandrel Expansion beyond Zircaloy tube Inner Radius.

By assuming that the original gap size is 0.2 mm, the gap size expansion as a consequence of mandrel expansion beyond zircaloy inner radius is calculated with eq. (28) and eq. (29). These values are plotted in Fig. 12. The gap expansion depends on mandrel expansion and zircaloy tube temperature. In this figure, the gap expansion by plastic deformation is about 17% at 700°C and 0.9% mandrel expansion beyond zircaloy inner radius.

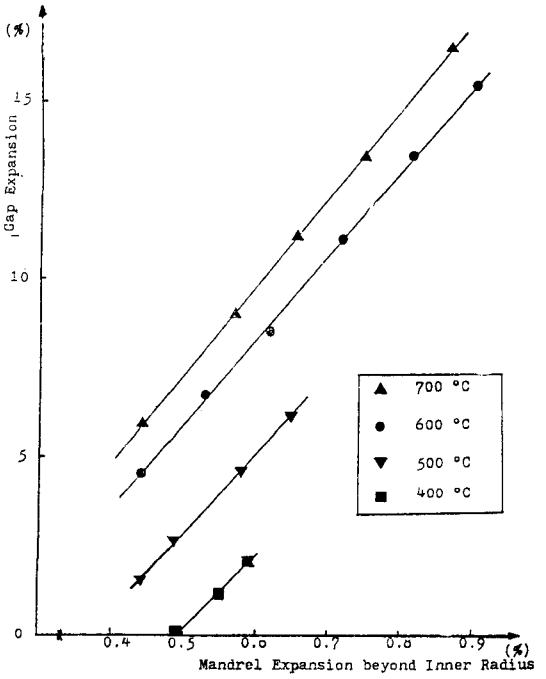

Fig. 12. Gap Expansion vs. Mandrel Expansion beyond Zircaloy-4 Tube Inner Radius

From design criteria, the hoop strain of zircaloy clad is maintained below 1% of its steady state diameter. This value is equivalent to about 23% of gap expansion. The criterion

seems much more conservative than the present experimental results.

But if mandrel expansion exceeds over 1.2% beyond zircaloy inner radius at 700°C during steep power change, the gap expansion might exceed the design criteria.

If the test is proceeded with internal gas pressurization method, this uniform gap expansion measurement is difficult because of local plastic instability. So in relation with gap expansion estimation, this simple mandrel expansion test method has its superiority.

IV. 5. The Gap Expansion vs. Zircaloy Clad Temperature under Constant Mandrel Expansion.

To study the zircaloy tube wall temperature effect on gap expansion, the gap expansion is plotted with zircaloy tube wall temperature at the 0.55% of mandrel expansion in Fig. 13.

This results indicate that the gap expansion has linear proportional behavior to zircaloy tube temperature for 400—600°C range. The incremental rate of gap expansion decrease over 600°C. This behavior coincides with the temperature dependence of zircaloy yield stress.

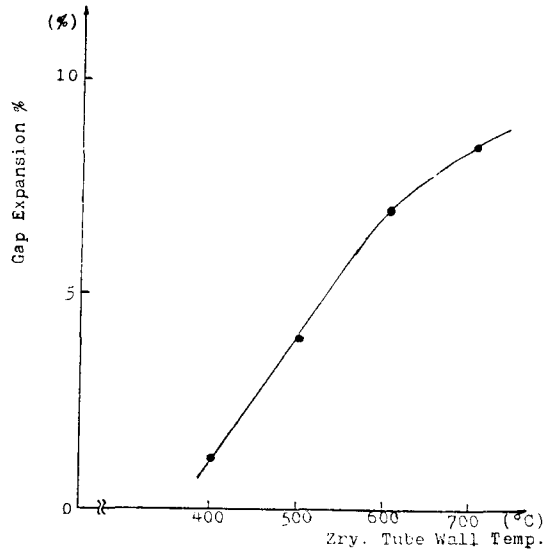

Fig. 13. Gap Expansion % vs. Zry. Tube Temp. under 0.55% Mandrel Expansion

V. Conclusions

The experimental conclusions are as follows;

(1) Zircaloy-4 tube yield pressure and yield stress decrease linearly with temperature in the range of 400—600°C. Above 600°C, the decreasing rate is reduced.

(2) The activation energy of yielding under constant strain and strain rate is 10.75KJ/mole for 400—474°C and 26.06KJ/mole for 474—700 °C. Therefore the yielding mechanism of zircaloy-4 tube is changed at that temperature.

(3) The pellet-clad gap expansion by plastic deformation of zircaloy clad is about 17% at 700°C and 0.9% mandrel expansion. From the design criteria of 1% hoop strain, the calculated gap expansion is about 23%, If mandrel or uranium-dioxide pellet expansion exceeds over 1.2% beyond zircaloy inner radius at 700°C temperature by steep power excursion, the gap expansion might exceed the design criterion.

(4) For the zircaloy clad yielding and pellet-clad gap expansion study, this simple mandrel expansion test method and the derived mathematical equations prove to be a reliable and simple technique.

Reference

1. H.M. Chung et al., "Deformation and Rupture Behavior of Zircaloy Cladding under Simulated LOCA Conditions", Zirconium in the Nuclear Industry, ASTM STP 633, 1977.
2. H.M. Chung et al., "Development of an Oxygen Embrittlement Criterion for Zircaloy Cladding Applicable of LOCA Accident Conditions in LWR", Zirconium in Nuclear Industry, ASTM STP 681, 1979.
3. EPRI NP-526, Vol 4. Part 1, Transient Deformation Property of Zircaloy for LOCA Simulation, Final Report, May, 1980.
4. A. Puill et al., "Irradiation in the CAP Reactor

of FRAGEMA Fuel Assemblies under Power Transients Representative of Super Imposed Load Follow and Remote Control Regimes", IAEA Specialists' Meeting on Power Ramping and Cycling Behavior of Water Reactor Fuel, in Petten, the Netherlands, Sep. 8th & 9th, 1982.

5. Steinar, "The Effect of Load-Following Operation on Fuel Rods", Nucl. Eng. & Des. 33(1975) 261-269.
6. J.T.A. Roberts et al., "On the Pellet-Cladding Interaction Phenomenon", Nucl. Tech. Vol. 35, Mid-August 1977.
7. H.M. Chung et al., "Fracture Behavior and Microstructual Characteristics of Irradiated Zircaloy Cladding", The 7th International Conference on Zirconium in the Nuclear Industry, Strasbourg, France, June 24-27, 1985.
8. H.M. Chung, "Phase Transformations in Neutron-Irradiated Zircaloys", The 13th International Symposium on Effects of Radiation on Materials, Seattle, Washington, June 23-24. 1986.
9. J.T.A. Roberts, Structual Materials in Nuclear Power System. Plenum Press, 82-85, 1981.
10. Y.S. Touloukian, Thermophysical Properties of High Temperature Solid Materials. Vol. 1 Elements, Purdue University, 462-463, 1967.
11. D.L. Hagrman et al. MATPRO-VERSION 11, A Handbook of Materials Properties for Use in the Analysis of LWR Fuel Rod Behavior, EG & G Idaho, Inc. 240-270, 1979.
12. A.C. Ugural, S.K. Fenster, Advanced Strength and Applied Elasticity, Elsevier, 238-239, 1981.
13. EPRI NP 567, Development of the Materials Code. MATMOD (constitutive eqs for zircaloy), 4-20 Dec. 1977.
14. D.R. Olander, Fundamental Aspects of Nuclear Reactor Fuel Elements, Technical Information Center Energy Research and Development Administration, 426-427, 1976.
15. A. Terens et al. "Stress Corrosion Cracking of Zircaloy-4 Cladding Tubes (threshold in presence of iodine)", J. of Nucl. Materials 126 (1984) 91-102.
16. G.E. Dieter, Mechanicl Metallurgy, 2nd ed., Mc-Graw Hill, 353-357, 1976.